

Modern silica sinter deposits from an island-arc setting and their potential for fossilizing plants

Aya Kubota ^{a,1}, Ryo Taniguchi ^{b,1}, Tomoyuki Ueda ^{c,1}, Yasuhiro Iba ^{c,1,*}

^a Research Institute for Geo-Resources and Environment, Geological Survey of Japan, National Institute of Advanced Industrial Science and Technology (AIST), Tsukuba 305-8567, Japan

^b School of Biological Sciences, University of Edinburgh, EH9 3BF, UK

^c Department of Earth and Planetary Sciences, Hokkaido University, N10W8, Kita-ku, Sapporo 060-0810, Japan

ARTICLE INFO

Editor: H. Falcon-Lang

Keywords:
Silica sinter
Hot spring
Island arc
Forest
Fossilization
Lagerstätten

ABSTRACT

Silica sinters deposited by hot-spring activities form Lagerstätten with numerous three-dimensional, cell-preserved fossils. The formation processes and depositional facies of silica sinters have been documented in large-scale geothermal provinces, including mantle-plume hotspots and mid-ocean ridges. Silica sinters in these areas preserve plants and microbes which are adapted to survive under geothermal stress, and which live inside the hot-spring system. Most plants are, however, intolerant to this specific environment. They are growing outside the hot springs, their chance for being embedded and preserved in the silica sinters is thus limited. Paleodiversity estimates and paleoecological reconstructions of past silica sinter Lagerstätten are therefore considered to be ambiguous. Here, we present a new depositional facies model of silica sinter from a forested island-arc setting, and discuss the taphonomy of richly preserved plants from these settings. At Nakabusa Hot Springs in central Japan, numerous small seep points emerge on densely forested slopes, where they form silica sinters. These sinters are characterized by the incorporation of abundant modern plants and insects from the adjoining forests, in addition to temperature-specific microbes. Because narrow channels flow down steep slopes with little disturbance of the forests, a distinctive bio- and lithofacies has developed that richly preserves the present-day native vegetation. The facies model presented here can serve as a valuable modern analog for better understanding the depositional processes of plant-rich fossil silica sinters. It may further help to understand the factors controlling the fossilization of land-based vegetation, thereby improving its relevance for interpretations throughout the geologic record.

1. Introduction

Siliceous hot-spring deposits are formed by silica precipitation from geothermal water discharged at the ground surface and lake floor (e.g., Renaut et al., 2002; Campbell et al., 2015a). The occurrence of abundant fossils with exceptional three-dimensional preservation in silica sinter has promoted extensive paleobiological and geobiological investigations (e.g., Konhauser et al., 2003; Guido et al., 2010; Guido and Campbell, 2011; Channing, 2018). The Rhynie chert (Early Devonian) for example, one of the most important fossil Lagerstätten, is a hot-spring silica sinter deposit. It preserves numerous fossils of plants, arthropods, and fungi, enabling the reconstruction of one of the earliest terrestrial ecosystems

(Trewin and Rice, 2004; Channing, 2018; Edwards et al., 2018; Strullu-Derrien et al., 2019; Garwood et al., 2020), thus shedding light on the colonization of the continents. Siliceous hot spring deposits have attracted interest for hosting and preserving extremophile microorganisms (Guido et al., 2019; Sagasti et al., 2024; Rowe et al., 2025). Recently discovered siliceous deposits on the planet Mars, which are morphologically similar to silica sinters on Earth, highlight their astrobiological significance (Squyres et al., 2008; Ruff and Farmer, 2016; Cady et al., 2018).

Recognizing their broad scientific importance, field-based investigations have clarified the formation processes of silica sinter in large-scale geothermal-hydrothermal provinces; they are positioned on

* Corresponding author.

E-mail addresses: a.kubota@aist.go.jp (A. Kubota), v1rtanig@ed.ac.uk (R. Taniguchi), tomtom980101@eis.hokudai.ac.jp (T. Ueda), iba@sci.hokudai.ac.jp (Y. Iba).

¹ These authors contributed equally to this work.

mantle-plume hotspots (Yellowstone National Park, USA; Hurwitz and Lowenstern, 2014), continental rifts (Taupō Volcanic Zone, New Zealand; Lynne and Campbell, 2004), mid-ocean ridges (Iceland; Tobler et al., 2008), and continental arcs (El Tatio Geyser Field, Chile; Fernandez-Turiel et al., 2005). In a widely accepted depositional model, hydrothermal discharge produces ca. 100-m-scale landforms associated with silica sinter, including geysers, vent pools, conical mounds, aprons, terraces, and geothermally influenced wetlands (Campbell et al., 2015a; Channing, 2018; Hamilton et al., 2019). Large-scale hot-spring systems form extreme environments for most living organisms. The vent-to-distal thermal gradient only allows distinct micro-biotic assemblages to settle. Thermophilic bacteria dominate the near-vent high-temperature sector, whilst mesophilic cyanobacteria colonize the intermediate zone (Campbell et al., 2015a, 2015b). Only those plants and grasses which tolerate the geothermal stress survive in the distal low-temperature area (Channing and Edwards, 2009b, 2013). These hot-spring assemblages are buried by silica sinter via progressive silicification (Channing and Edwards, 2009a; Campbell et al., 2015b). Most plants are, however, intolerant to these stressful environmental conditions. They only grow outside the individual hot-spring system, having a low preservation potential (Channing and Edwards, 2009b, 2013).

Large-scale silica sinters therefore rather preserve assemblages living inside the hot-spring system than those from outside. Paleodiversity estimates and paleoecological reconstructions, which are based on assemblages from these silica sinters, are therefore thought to be strongly biased (Channing and Edwards, 2013).

Island-arc settings along the eastern Eurasian margin are characterized by high-relief mountainous terrains with numerous small-scale geothermal fields which are generated by subduction-related orogeny and volcanic activity (Taira, 2001; Matsumoto et al., 2022). Forests are well-developed in this area under abundant rainfall caused by the East Asian monsoon (Kira, 1991). Here, the seepage of thermal water occurs in the forested slopes. The silica sinters in these areas contain numerous plant remains from the forests covering the sites. Research of the localities has been limited to mineralogical and microbiological surveys over the last hundred years (e.g., Suzuki, 1889; Sato, 1922; Akahane et al., 1997). The sedimentological characteristics of silica sinter remain therefore largely unknown. This study presents a detailed analysis of the typical, modern silica sinter deposits in central Japan, to elucidate their depositional facies, formation processes, and the taphonomy of the biota preserved.

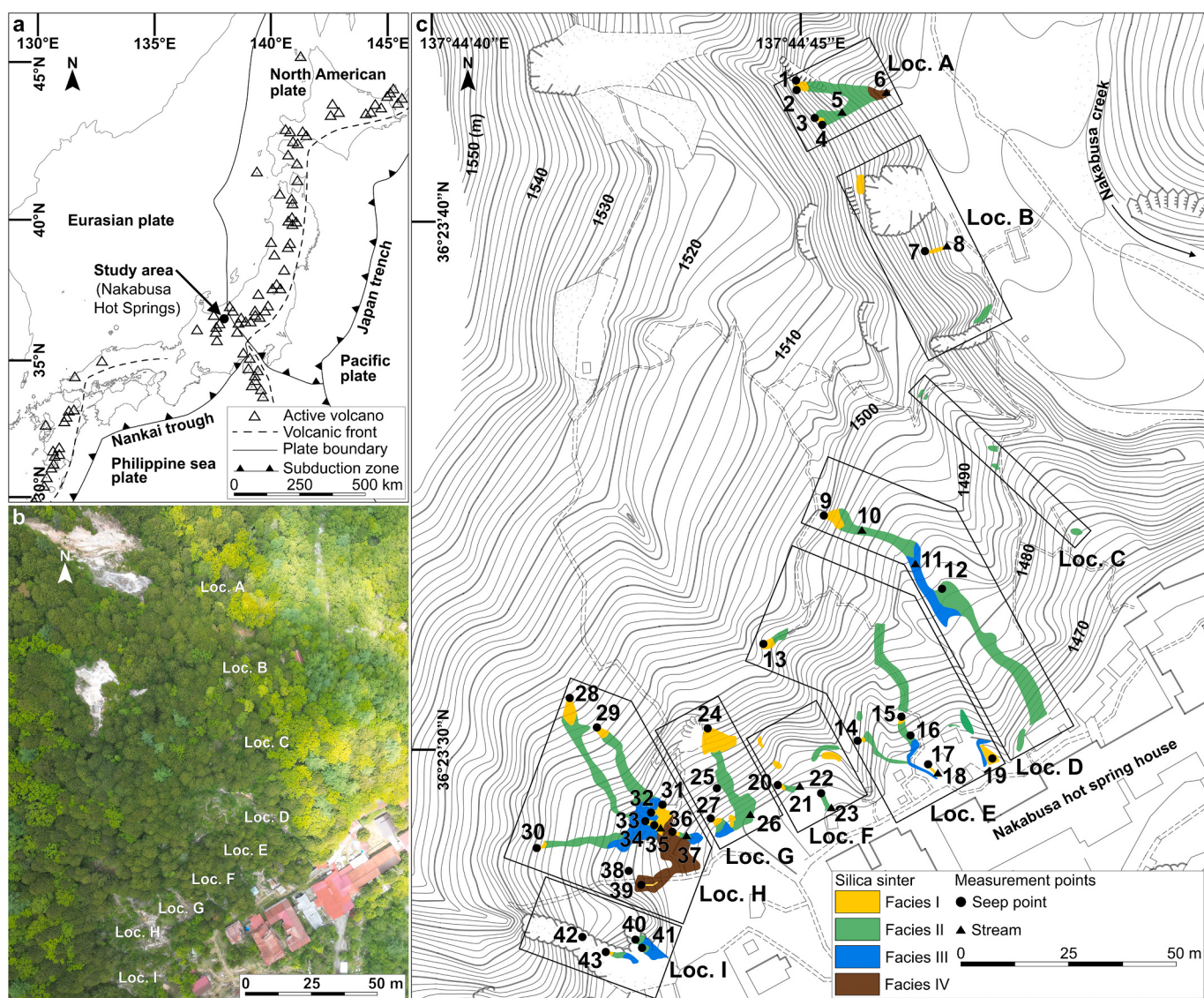


Fig. 1. Locality map and distribution of silica sinter in the study area. **a.** Location of Nakabusa Hot Springs, Azumino City, Nagano, central Japan. Map is modified from Nakada (2017). **b.** Aerial photograph of the forest-covered study area. **c.** Distribution of seep points and silica sinter deposits.

2. Geological and environmental settings

The northeast-southwest-trending volcanic front of eastern Japan is formed along the subduction of the Pacific Plate underneath the North American Plate (Fig. 1a). Nakabusa Hot Springs are situated near the western end of the volcanic chain in Azumino City, Nagano, central Japan at elevations of 1450–1560 m a.s.l. (36°23'39" N, 137°44'48" E; Fig. 1). The Shinanozaka Fault, an active fault oriented northwest to southeast, underlies Nakabusa Hot Springs (Kato and Sato, 1983). The base rocks in the study area are composed of the latest Cretaceous to earliest Paleogene granitic intrusions (Kato and Sato, 1983). In the southern and eastern parts of the study area, Nakabusa Creek and its branches form a series of small incised valleys. Their steep slopes are covered by dense forests (Fig. 1b). Hydrothermal seeps and silica sinter outcrops occur sporadically on the slopes (Figs. 1b, 2). Nakabusa silica sinter was designated a Japanese Natural Monument in 1928, and most outcrops remained therefore well protected from anthropogenic disturbance.

The local climate is characterized by significant seasonal temperature contrasts and high annual precipitation. Long-term monthly means range from -12.4 °C in January to 24.5 °C in August. Mean monthly precipitation varies from 99.2 mm in February to 242.4 mm in July, providing an annual average of 1811.9 mm. Flood events have not been recorded in the Nakabusa Hot Springs over the past 200 years (personal communication with the site owner), including our field survey in 2019–2025. Average maximum snow depth reaches 172 cm in March (MLIT, 2022). The slopes are covered by natural subalpine coniferous forests dominated by Japanese cypress (*Chamaecyparis obtusa*), with Japanese oak (*Quercus crispula*), bamboo grass (*Sasa veitchii*), staghorn clubmoss (*Lycopodium clavatum*), mosses and other taxa (Figs. 1b, 2). Snow does not accumulate in winter within the hydrothermal channels, which support perennial microbial mats composed of chemolithotrophic bacteria, cyanobacteria, and green photosynthetic bacteria (Nakagawa and Fukui, 2002; Kubo et al., 2011; Everroad et al., 2012).

3. Methods

In the field, the seep points and silica sinter outcrops were identified and mapped (Fig. 1c); the temperature, pH, and dissolved silica concentration of water were measured on site. Silica concentration was quantified by the molybdenum blue method using a silica colorimeter

(HI97770C; Hanna Instruments Ltd.). At each outcrop, we described the distribution patterns and sedimentary structures of the sinter, including an account of the coexisting biota. The bio- and litho-facies of the sinters was classified based on these analyses. Microstructures of sampled silica sinters were observed via transmitted-light optical microscopy and a scanning electron microscope (JSM-6510; JEOL Ltd.). To estimate the sinter growth rates, ceramic tiles (108 × 60 × 10 mm; Nittai Kogyo Co., Ltd.) were placed at 16 points on the slopes facing south (highly insolated; Loc. E) and east (shaded; Loc. B) (Fig. 1c; Supplementary table S1, S2). At some localities, tiles were positioned under two different experimental conditions, exposed to water spray and fully submerged in the flow channels. All tiles were collected after approximately 3 or 9 months. The silica growth rate (mm month⁻¹) was calculated from the precipitation thickness on each tile.

4. Results

4.1. Overview of the hydrothermal environment

Thermal water is discharged from discrete seep points on forested slopes, generating shallow, narrow, and elongated channels (depth: 0.1–1 cm; width: 0.6–16.2 m; length: 2.0–56.0 m), along which silica sinters develop (Figs. 1c, 2). A total of 32 seep points were identified from nine areas (Locs. A–I), their diameters are less than 10 cm each (Figs. 1c, 2, 3a). Water seeping is gentle at most points, only a few seeps disperse a sporadic thermal spray reaching approximately max. 30 cm in height and 50 cm in radius (measurement point no. 33 in Fig. 1c). No geysers exist within the study area. Water temperatures at the seep points range from 53.1 to 97.5 °C (Supplementary table S1). The pH values indicate predominantly alkaline conditions (pH 7.57–9.47) with four exceptions (nos. 1, 22, 25, and 42 in Fig. 1c) showing near-neutral pH (6.60–7.36) (Supplementary table S1). Both temperature and pH were stable throughout the year (Supplementary table S1). Dissolved silica concentration at the seep points and in streams shows various values, ranging from 70 to 368 mg L⁻¹ (Supplementary table S1).

4.2. Growth rate of silica sinter

At Loc. E on the south-facing slope, finely laminated siliceous coatings were formed on the experimental tiles exposed to thermal water spray, whereas no silica precipitated on the tiles submerged in the

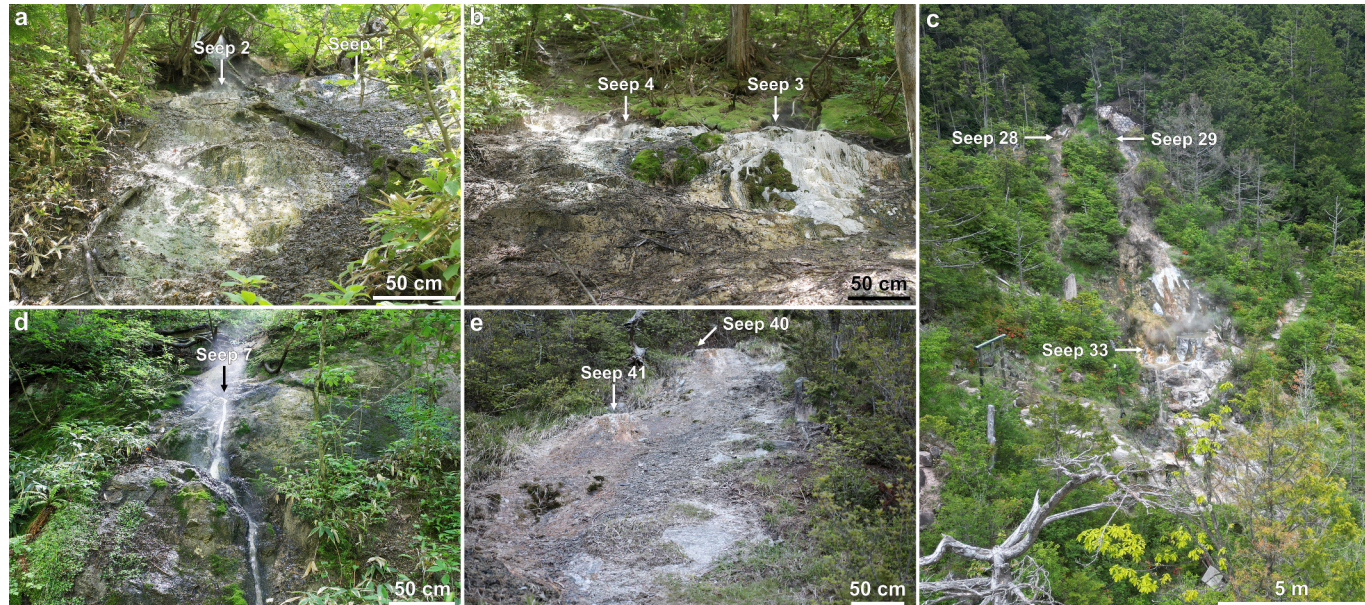


Fig. 2. General views of small-scale silica sinter deposits on forested slopes in the Nakabusa Hot Springs area. a, b. Loc. A. c. Loc. H. d. Loc. B. e. Loc. I.

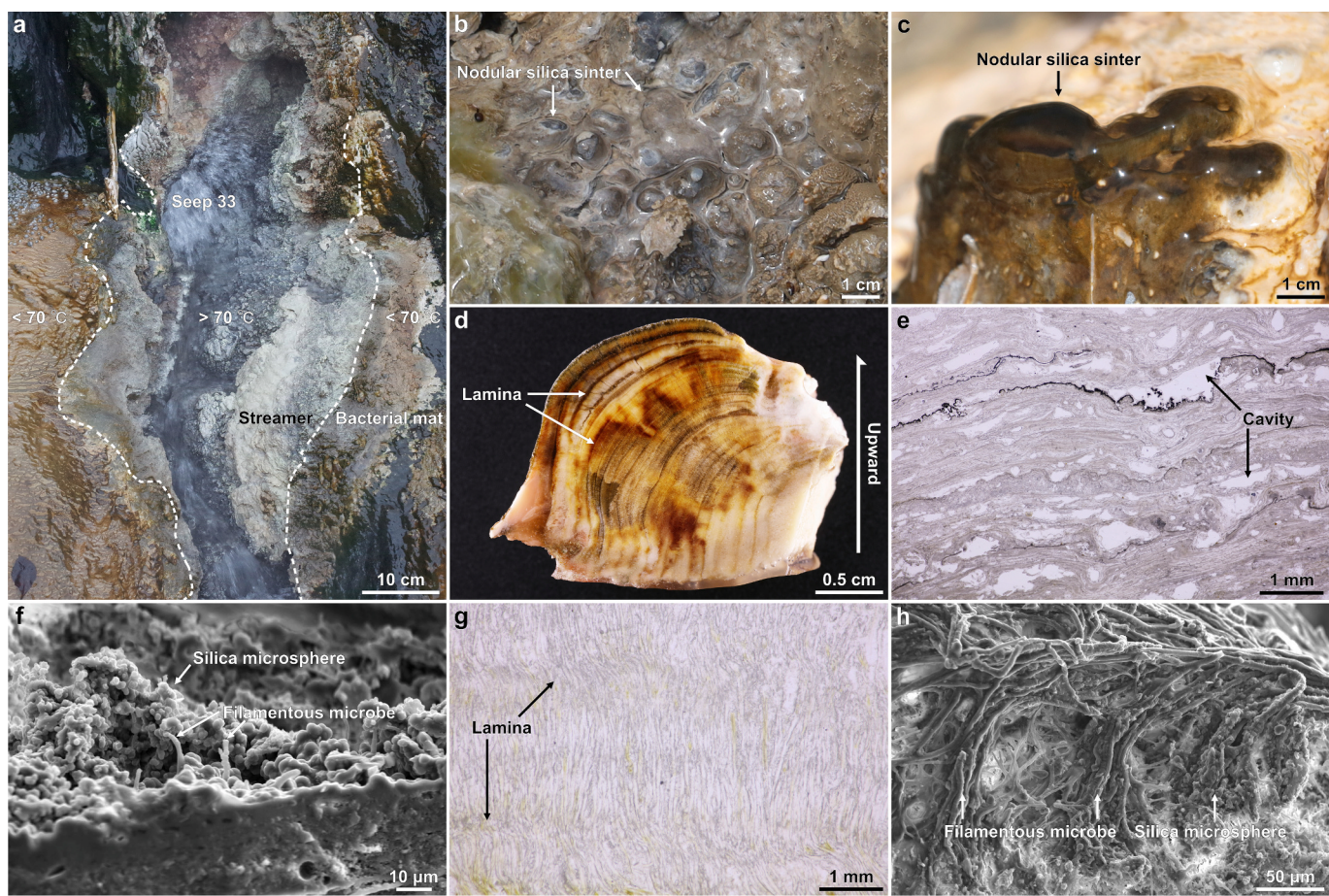


Fig. 3. Macro- and micro-textures of Facies I. a. Thermophilic bacterial mats near no. 33 at Loc. H. b–d. Nodular textures near no. 32 at Loc. H. d. Vertical section of the silica sinter of a nodule shown in Fig. 3c., displaying fine-laminated internal structures. e, f. Micro-textures of proximal area of Facies I at the no. 24, Loc. G. g. Fine-laminated internal structures with cavities. f. Silica microspheres with filamentous microbes. g, h. Micro-textures of the marginal area of Facies I near no. 7 at Loc. B. Concentrations of filamentous microbes oriented perpendicular to the laminae.

channels. The tiles at Loc. B on the east-facing slope also showed no silica growth; instead, they were covered by a bacterial mat approximately 0.1 mm thick (Supplementary table S2). Based on the measured coating thickness, the maximum sinter growth rate was calculated as $0.78 \text{ mm month}^{-1}$ (Loc E; Supplementary table S2).

4.3. Bio- and litho-facies

The silica sinter encountered in the study area is subdivided into four facies (I–IV; Figs. 1c, 3–5). The sinter is markedly more developed on the south-facing slope than on the east-facing one (Fig. 1c). Some sinters in Locs. B–H were no longer connected to their source channels and silica deposition had ended. They are now buried under the soil. These relict sinters are occurring in all of the four types of facies, which are described in detail further down.

4.3.1. Facies I (Fig. 3)

Distribution: This facies occurs at elevations $\leq 1507 \text{ m}$ on slopes with angles of $14.0\text{--}46.8^\circ$. It is distributed $0.0\text{--}9.0 \text{ m}$ downslope from seep points (Fig. 1c). The sinter bodies exhibit a fan-shape with the seep point as the apex; their length is $1.2\text{--}9.0 \text{ m}$ and the distal width is $0.6\text{--}9.5 \text{ m}$. The area covered by sinter is $1.1\text{--}19.8 \text{ m}^2$ ($N = 14$), the smallest of all four facies (Fig. 1c).

Depositional environment: Water temperature is $58.0\text{--}97.5 \text{ }^\circ\text{C}$, and pH is $6.60\text{--}9.47$ for this facies ($N = 27$; Supplementary table S1). In the proximal part ($> 70 \text{ }^\circ\text{C}$), white, gray, and black thermophilic bacterial streamers coat the sinter surface (Fig. 3a). In the marginal area

($\sim 50\text{--}70 \text{ }^\circ\text{C}$), green to orange thermophilic bacterial mats develop (Fig. 3a). Vegetation is locally absent within a few meters around each seep point, resulting in small input of plants and animals to the sinter.

Lithology: Facies I overlies the granitic bedrock as siliceous deposits, it is up to 10 cm thick and exhibits a nodular relief (Figs. 3b–d). The deposit is finely laminated and contains silicified bacteria (Figs. 3d–h). Proximal to the seep, in the high-temperature zones ($> 70 \text{ }^\circ\text{C}$), finely laminated silica layers (a few micrometers thick) with cavities (tens of micrometers to 1 mm in diameter) are developed and sparse filamentous bacteria are incorporated (Fig. 3f). More distal, in the lower-temperature zones ($< 70 \text{ }^\circ\text{C}$), densely packed bacterial remains are laminated tens to hundreds of micrometers apart (Fig. 3g). These filaments are oriented perpendicular to the laminae and are either infilled or encrusted by partially cemented silica microspheres ($< 5 \mu\text{m}$ in diameter) (Figs. 3g, h).

4.3.2. Facies II (Fig. 4)

Distribution: This facies occurs at elevations $\leq 1505 \text{ m}$ on slopes of $6.3\text{--}49.6^\circ$. It is distributed $0.0\text{--}47.8 \text{ m}$ downslope from seep points (Fig. 1c). The sinter bodies have an elongated shape; their length is $2.0\text{--}47.8 \text{ m}$, their width is $2.0\text{--}6.9 \text{ m}$, and the covered area is $3.3\text{--}183.9 \text{ m}^2$ ($N = 17$).

Depositional environment: Water temperature is $28.0\text{--}92.1 \text{ }^\circ\text{C}$, and pH is $6.66\text{--}9.44$ ($N = 11$; Supplementary table S1). Thermal water channels lie beneath a dense forest canopy, supplying abundant plant debris to the sinter surface (Figs. 2a–c). Both woody and herbaceous plants grow along channel margins (Figs. 2a, b). Mosses form patches in small interchannel areas (Figs. 4a, i–k).

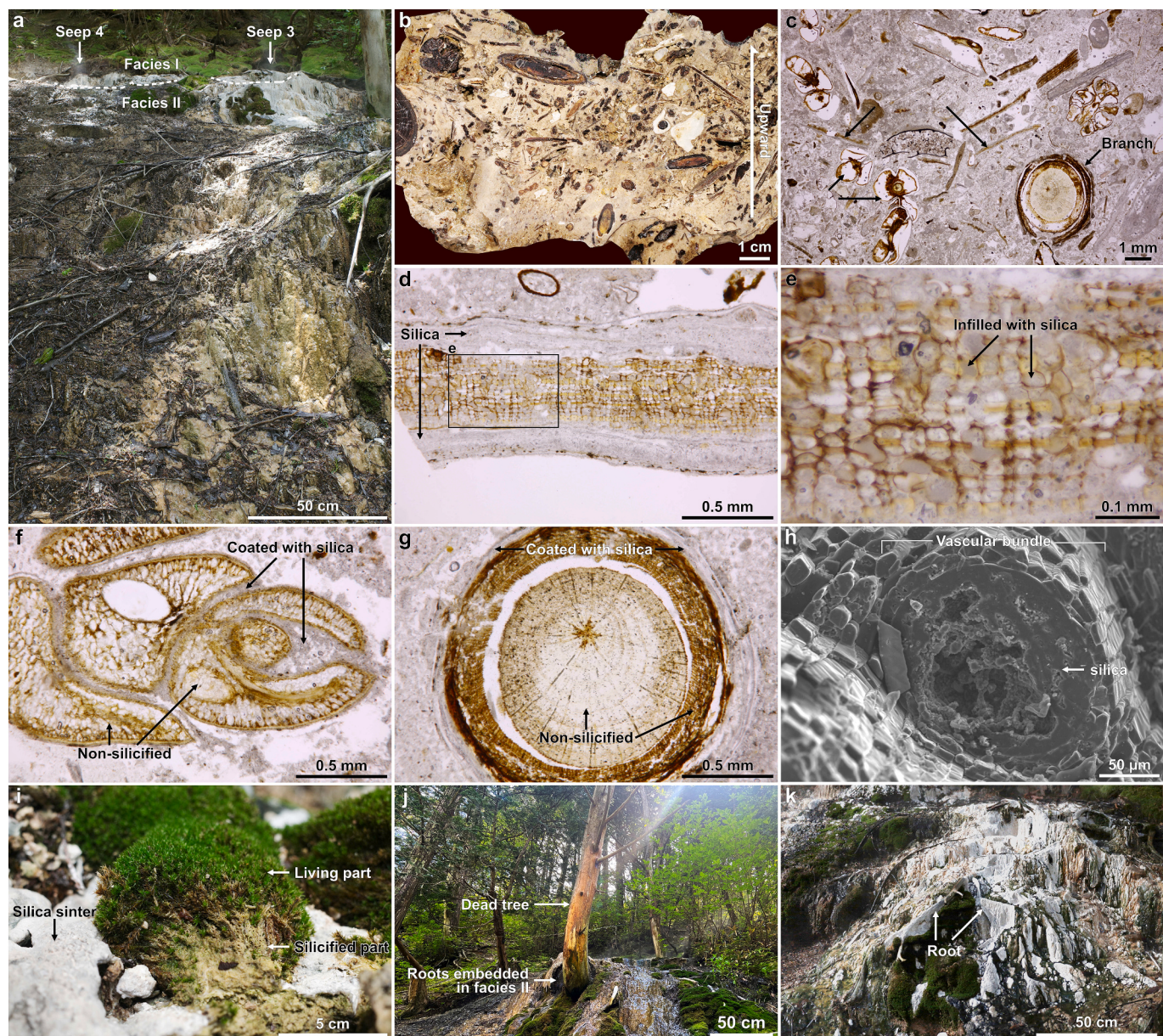


Fig. 4. Macro- and micro-textures of Facies II. a. General view of Facies II at Loc. A, characterized by a woody-debris-jam-like framework. b. Vertical cross-section of a slab from Loc. A. Abundant plant remains embedded in silica sinter. c–g. Photomicrographs of samples from Loc. A. d. Transverse section of a broadleaf-tree leaf. e. Close-up of Fig. 4d. Cells infilled with silica. f. Oblique section of a shoot of *Chamaecyparis obtusa* coated with silica. g. Cross section of a twig coated with silica. h. Fractured surface of a broken twig infilled with silica. i–k. In situ occurrence of plants. i. Moss showing a hybrid state; living apices and silicified base. j. Standing deadwood (*C. obtusa*) embedded in silica sinter. k. Root collar almost completely buried by silica sinter.

Lithology: Facies II is characterized by abundant plants cemented by silica (Figs. 4a–c), it also includes granite clasts, green to orange bacterial mats, insect remains, and reworked sinter clasts derived from Facies I (< 1.5 cm in diameter). The various plant remains from the surrounding forests form a woody-debris-jam-like framework, increasing the thickness of the silica sinter up to 20 cm in maximum thickness (Figs. 4a, b). The plant assemblages are composed of shed organs: conifer needles, shoots, cones, bark fragments, broadleaf-tree leaves, and fruits, primarily derived from trees right over the sinter (Figs. 4a–c).

Preservation modes of the plant remains generally differ according to the plant organs and the taxonomy of the individual specimens. Remains such as broadleaf-tree leaves with thin cuticles, are fully permineralized; their cells are completely infilled by aggregated silica microspheres (~2 µm in diameter) (Figs. 4d, e). Remains such as twigs, conifer shoots and

cones with well-developed cuticles or lignified tissues on the other hand, mainly exhibit surface silica coating, with internal cells remaining unfilled (Figs. 4f, g). Even among the latter, partially broken plant remains show internal silica precipitates which have already undergone silicification (Fig. 4h). In addition to these plant remains, Facies II contains in situ trees and mosses, some of the latter show a hybrid condition (Fig. 4i). In some gametophores the apical part is still living, while its base is already silicified (Fig. 4i). The trees in the channel are dead but still standing upright, and their root collars are embedded in the silica sinter (Figs. 4j, k).

4.3.3. Facies III (Figs. 5a–d)

Distribution: This facies occurs at elevations <1489 m on slopes of 13.6–37.7°. It is distributed 2.0–69.0 m downslope from seep points (Fig. 1c). The sinter bodies have an elongated shape; their length is

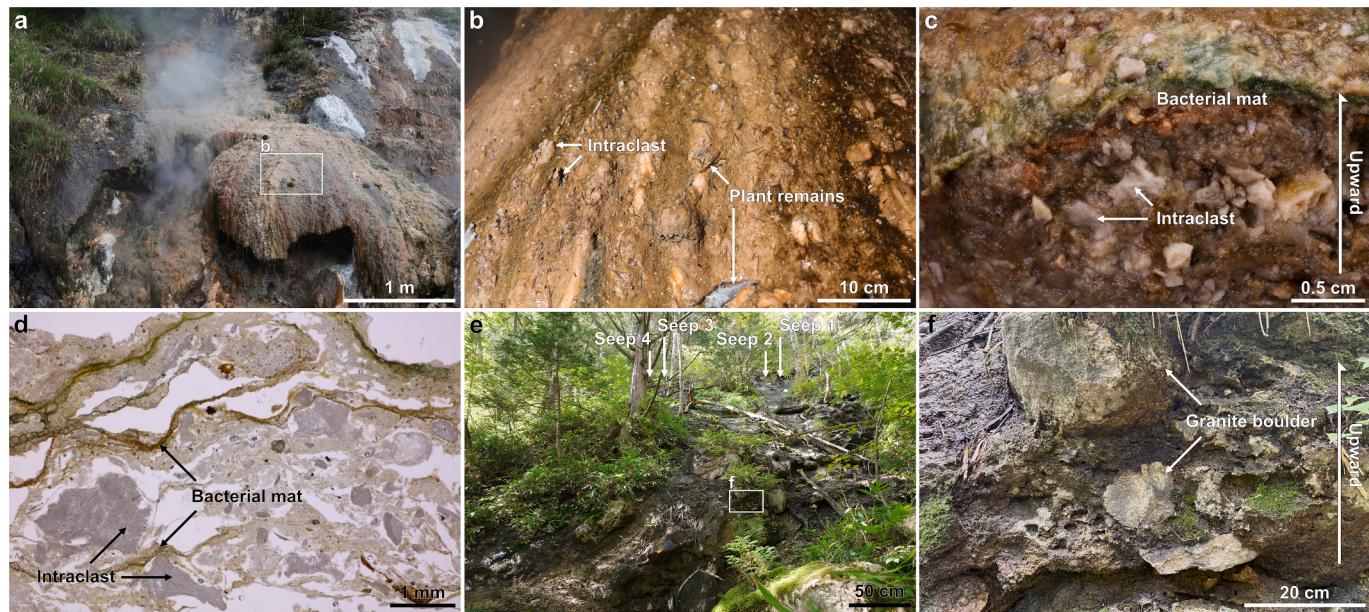


Fig. 5. Macro- and micro-textures of Facies III and IV. a-d. Facies III. a. General view of Facies III at Loc. H. Non-silicified bacterial mats are well developed along a water temperature gradient. b. Close-up of Fig. 5a. Small plant remains and reworked sinter clasts trapped by bacterial mat. c. Vertical section of a thick bacterial mat with reworked clasts. d. Internal structures of Facies III. e, f. Facies IV. e. General view of Facies IV at Loc. A. f. Close-up of Fig. 5e. Landslide deposits cemented by silica and upstream-derived clasts.

4.1–23.4 m, the width is 2.0–16.2 m, and the covered area is 6.0–90.6 m² ($N = 8$) (Fig. 1c).

Depositional environment: The water temperature is 29.5 °C, and the pH is 8.57 (Supplementary table S1). Green to orange mesophilic bacterial mats (up to 2 mm thick) are common along the thermal channel (Fig. 5a). Vegetation is present along the channel margins, but less well developed than in Facies II.

Lithology: Facies III is primarily composed of layered, non-silicified bacterial-mat laminae (Fig. 5c). Both the surfaces and the interlaminar zones of the sinter trap granite clasts and reworked sinter clasts are derived from Facies I and II, each less than 1.5 cm in diameter (Figs. 5b-d). The laminae capture plant remains such as conifer shoots, small twigs, and broadleaf-tree leaves (Fig. 5b). Most plant remains in Facies III are non-silicified, they are sparse, and small in scale and do not form a woody-debris framework. The maximum thickness of the deposits is ~50 mm.

4.3.4. Facies IV (Figs. 5e, f)

Distribution: This facies occurs at elevations ≤1486 m on slopes of 20.7–27.2°. It is distributed 24.9–56.0 m downslope from seep points (Fig. 1c). The shape of the sinter bodies is broad, its distal margin reaches the slope–flat interface. The length is 6.6–15.6 m, proximal width is 4.7–7.7 m, and the covered area is 14.5–81.7 m² ($N = 2$) (Fig. 1c).

Depositional environment: The water temperature in the flow channel at Loc. A is 21.5 °C (Supplementary table S1). Here, the channel margins host a well-developed vegetation (Fig. 5e), whereas the area surrounding Loc. H lacks any plants.

Lithology: Facies IV comprises silica-cemented landslide deposits. It contains granule- to boulder-sized clasts exhibiting inverse-grading, reworked sinter clasts derived from Facies I–III, and plant fragments (twigs, bark, and stems) (Fig. 5f). The maximum thickness is ~2 m.

5. Discussion

5.1. Factors controlling the growth of silica sinter

Under subaerial conditions, the drivers of silica precipitation are temperature declines, pH shifts, and evaporative concentration of

dissolved silica, dominantly controlled by cyclic wetting and drying (Braunstein and Lowe, 2001; Lynne et al., 2019). The specific drivers of these wet-dry cycles depend on the unique geothermal and environmental systems at each hot-spring setting. The controlling parameters include strong temperature gradients (White et al., 1956), wind-driven evaporation (Nicolau et al., 2014), wave and splash action (Braunstein and Lowe, 2001; Mountain et al., 2003), and capillary rise and diffusion (Lynne et al., 2019).

Our field observations and experiments suggest that solar-driven evaporation is the principal factor controlling subaerial sinter growth in the study area. Silica sinter developed most abundantly on the highly insolated south-facing slope, whereas it is sparse and small in shaded and east-facing positions (Fig. 1c). At the highly insolated site, the sinter is actively formed even with low silica concentration (70 mg L⁻¹ in no. 27, Loc. G); in contrast, the silica deposition is thin at the shaded area with high concentration (344 mg L⁻¹ in no. 7, Loc. B). Silica deposits mainly along the channel margins and is not precipitated on the channel bed. These patterns were also observed in the tile experiments (Supplementary table S2). These findings indicate that frequent wet-dry cycles, enhanced by direct solar exposure, maximize silica deposition, rather than subaqueous precipitation of amorphous silica. Sinter in the study area develops along narrow and shallow streams on a steep, forested slope with a complex topography (Figs. 1c, 2, 6). These narrow and shallow channels would efficiently promote cooling. Although seepage is gentle, spray occurs from the streams on the uneven slope surfaces, subsequently accelerating the wetting-drying cycles. Previous studies have focused on microbial effects on silica sinter formation, such as providing nucleation sites for silicification (e.g., Konhauser et al., 2001). In the study area, the thick mesophilic bacterial mats of Facies III hinder evaporation and sinter formation with their high water-retention capacity (Locs. D, E, G–I), indicating a negative effect of microbes on silica deposition.

Across the steep forested slope of the study area, Facies I–IV are arrayed downslope in ascending order (Figs. 1c, 6). The hydrothermal water is discharged from individual seep points and flows downhill in narrow and shallow streams (< 5 m wide; 0.1–1 cm deep), without forming large geysers, pools, and sinter aprons/terraces. These small channels minimize the lethal hydrothermal effects for the surrounding

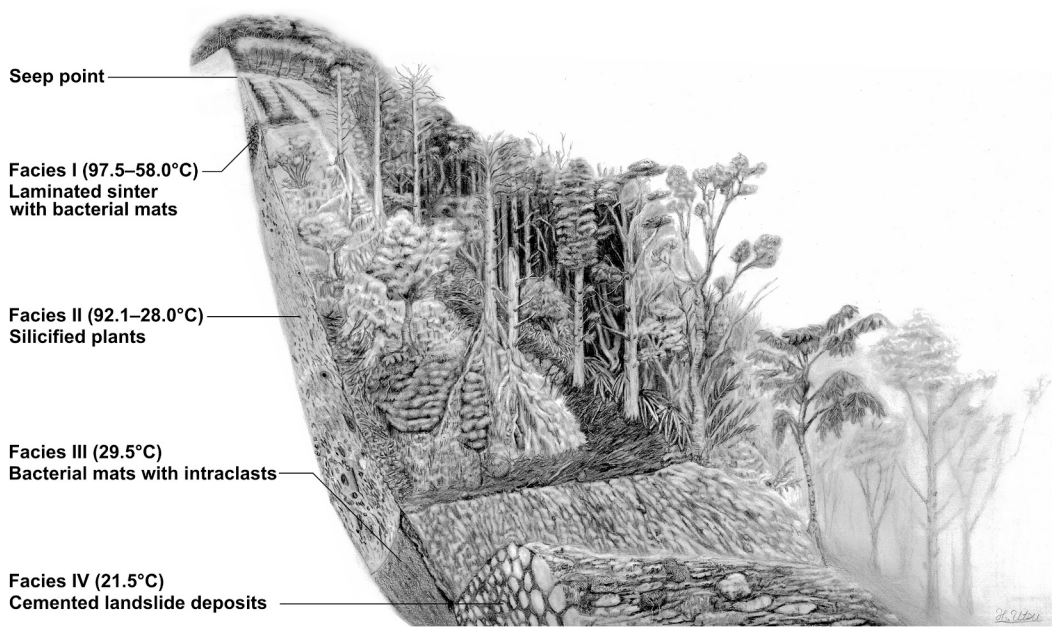


Fig. 6. Schematic diagram of forested island-arc silica sinter in Nakabusa Hot Springs, central Japan. Silica sinter develops along narrow and shallow streams from small seep points on a steep, forested slope. Facies I–IV are distributed downslope, in ascending order. In Facies II, abundant plant remains are incorporated into the sinter.

forests, allowing plants to thrive continuously from the high-temperature proximal facies (II) to the cooler distal facies (III–IV). The components and sedimentary structures of each facies are controlled by the cm–meter scale variations of the biotic communities corresponding to the thermal gradients. In Facies I ($97.5\text{--}58.0^{\circ}\text{C}$), the silica deposits show a fine lamination due to the absence of plants and the dominance of thermophilic bacteria (Fig. 3). These sinters have nodular surface morphologies (Figs. 3b–d). In contrast, Facies II–IV are rather thick (1 cm to 2 m in thickness), caused by the incorporation of shed organs, granite clasts, and reworked sinter clasts. Compared to the relatively smooth sinter surfaces of Facies I, the woody-debris framework of Facies II easily traps and fixes additional remains and promotes their silicification (Figs. 2a, b, 4a). Plant remains incorporated into this framework are initially coated with silica individually. The cavities between the plant remains were cemented and filled with trapped clastic sediment particles in a later phase, becoming integral components of the debris jam. The *in situ* plants are also preserved in Facies II, as standing-dead tree roots and moss from the reticulate-interchannel area are embedded into the sinter (Figs. 4i–k). In Facies III (29.5°C), thick, non-silicified bacterial mats are well-developed in the mid-temperature channels (Figs. 5a–c). These mats trap and incorporate abundant upstream-derived clasts without forming woody-debris frameworks (Figs. 5b, c). Facies IV (Figs. 5e, f) is represented by typical landslide deposits, which are cemented by a silica matrix and upstream-derived clasts. In summary, the four facies assemblages and distribution patterns of silica sinter in the study area are controlled by the topographical and biological settings. These include steep slope morphology, small and sporadic hydrothermal discharge, and dense forests (Figs. 2, 6).

5.2. Characteristics and paleontological significance of silica sinter in island-arc forests

The depositional processes, the environment, and the distribution patterns of biota in silica sinter formations have been documented in large silicic geothermal provinces. These provinces include mantle-plume hotspots (Yellowstone National Park, USA; Braunstein and Lowe, 2001; Guidry and Chafetz, 2002; Hurwitz and Lowenstern, 2014; Churchill et al., 2021), mid-ocean ridges (Geysir, Iceland; Tobler et al.,

2008), continental rifts (Taupō Volcanic Zone, New Zealand; Campbell et al., 2001; Lynne and Campbell, 2004) or high-elevation arid settings in continental arcs (El Tatio Geyser Field, Chile; Garcia-Valles et al., 2008; Nicolau et al., 2014; Gong et al., 2021). The model proposed by previous studies is now widely accepted as the standard framework for sinter formation (Campbell et al., 2015a; Channing, 2018; Hamilton et al., 2019). At surging vents, conical mounds are built up via brecciation of the conduit walls and their subsequent cementation by silica (Garcia-Valles et al., 2008; Campbell et al., 2015a; Churchill et al., 2021), whereas non-surging vents generate rather planar meter-scale pools (Lowe and Braunstein, 2003; Campbell et al., 2015a). The overflow thermal water streams subsequently precipitate silica in the channels and on the flood plains by forming large siliceous aprons and terraces (Jones and Renaut, 2003; Campbell et al., 2015b; Channing, 2018). Laminated streamer sinters with numerous thermophilic bacteria are formed on mound surfaces ($\sim 100\text{--}70^{\circ}\text{C}$), and various cyanobacterial mats are developed and embedded in downstream sinter aprons ($\sim 75\text{--}40^{\circ}\text{C}$) (Campbell et al., 2015a, 2015b). Fluctuating conditions in hot-spring settings, such as decreases in temperature or temporary pauses in fluids, can shift the distribution of these microbial communities (e.g., Jones et al., 2003; Sagasti et al., 2024).

Large-scale hot-spring systems are extreme, hostile environments for most living organisms. The amount of plant growth is limited in geothermal environments (Channing and Edwards, 2009b, 2013). Plants are generally missing around vents and their margins with high temperatures, they are also absent on aprons with hard, nutrient- and moisture-poor sinter substrates (Channing and Edwards, 2009b, 2013). Below 40°C , pioneer mosses and lichens appear on dry apron surfaces, and grasses tolerant of alkaline, saline conditions form low-diversity communities in geothermal influenced marshes ($\sim 25^{\circ}\text{C}$; Channing and Edwards, 2009b). Most plants (e.g., lodge-pole pine forests in Yellowstone National Park), are stenothermal and intolerant to the specific hot-spring conditions, including high temperatures, alkalinity, high salinity, concentrations of heavy metals, and flooding linked to hydrothermal activity (Channing and Edwards, 2013). These plants grow outside the individual hot-spring system in the neighborhood, their potential for preservations is low. Silicification of these plants occur only sporadically through occasional incursions of thermal water (Channing

and Edwards, 2009a, 2009b). Hot-spring assemblages composed of microbes and plants, which tolerate geothermal stress, are preserved in the silica sinter. In large-scale hot-spring systems, plants from outside the system are rarely recorded, while those living inside are well-preserved in the sinters.

The Nakabusa silica sinter, is characterized by the inclusion of rich plant assemblages. In island-arc settings, subduction-related orogeny produces high-relief mountainous terrain, and hydrothermal discharge occurs in numerous small-scale geothermal fields (Taira, 2001; Matsumoto et al., 2022). In Japan, these geological parameters go along with forests of high diversity and biomass, the latter are well-developed due to abundant rainfall caused by the East Asian monsoon (Kira, 1991). Different to other extensive silica sinter deposits, the Nakabusa silica sinter in the island-arc tectonic setting reflects a specific scenario of dense forests and small hot-spring systems (Figs. 1b, 2, 6). The hydrothermal channels are narrow and do not disturb the growth of the surrounding forests, promoting the preservation of silica sinter enriched in plant remains, closely reflecting the regional flora which is typical in the subalpine zone (Figs. 2a–c). Fifteen silica sinter occurrences were reported from Japan and Taiwan so far (Sato, 1922; Ozaki, 1972). Most of them are also on steep, densely forested slopes, suggesting that the facies patterns of the Nakabusa Hot Springs may exist throughout the East Asian islands (Supplementary fig. S1).

Throughout their geological record of ~407 ma, silica sinters yield exceptionally well-preserved fossil assemblages, such as Rhynie, northern Scotland (Rhynie chert; Dryden Flags Formation, Lower Devonian; Channing, 2018; Strullu-Derrien et al., 2019), northeastern Australia (Upper Devonian to Lower Carboniferous; White et al., 1989; Walter et al., 1996), the Deseado Massif, southern Patagonia (Late Jurassic; Guido et al., 2010; Guido and Campbell, 2011), and Heilongjiang, northeastern China (Upper Cretaceous; You et al., 2024). Modern, large-scale silica sinters have therefore been used to understand the paleoenvironmental and taphonomic processes which led to the formation of past Lagerstätten (Channing, 2018). These modern sinters, however, mostly preserve hot-spring assemblages, plants from outside the hot-spring system are rare (e.g., transportation, thermal water floodings; Channing and Edwards, 2013). Paleodiversity estimates and paleoecological reconstructions of the floral assemblages of silica Lagerstätten, are therefore thought to be strongly biased (Channing and Edwards, 2013).

The Rhynie chert is one of the most important Lagerstätte, preserving micron-scale and three-dimensional anatomical details of the earliest terrestrial ecosystem (Channing, 2018). The fossil plant assemblages preserved in the Rhynie chert are thought to have experienced a strong preservational bias due to the factors discussed earlier (Channing and Edwards, 2013; Wellman, 2018). Although the facies distribution and depositional environment of the Rhynie chert remain unclear, it is thought to have formed in marginal, geothermally influenced marshes with partial evidence from traditionally well-known hydrothermal provinces (Channing and Edwards, 2009b). This reconstruction is based on the lack of sedimentological indicators of high-energy or large-scale hydrothermal activity, such as vent mounds and extensive aprons (Channing and Edwards, 2009b). The Windyfield chert (Dryden Flags Formation; Rice et al., 2002), a fossil site slightly younger than the nearby Rhynie chert, is considered to have been positioned closer to the vent center (Trewin and Kerp, 2017). This environmental reconstruction is supported by multiple sedimentary features which include botryoidal textures, interpreted as indicators for splash-zones at vent rims (Fayers and Trewin, 2003; Trewin and Kerp, 2017). The known extension of the Windyfield chert is, however, limited, the sinter-forming activity was presumably short-term and the geothermal influence was highly localized (Trewin and Kerp, 2017). Similar botryoidal formed silica sinters were also found around small seep points and slope channels with hydrothermal spray in our study area (Figs. 3b, c), demonstrating that such textures occur without large-scale hot-spring systems. The formation process of the silica sinter at Rhynie may have differed from the

classic broad, high-energy geothermal models (e.g., Yellowstone National Park). The island-arc sinter described here indicates that small-scale hydrothermal activity on steep forested slopes can preserve fossil assemblages reflecting the regional flora (Fig. 6). The forested island-arc silica sinter from Nakabusa indicates that sedimentary facies of silica sinter models are more diverse than previously thought. The detailed facies model from forested island-arc settings, presented here, offers a new modern analog for explaining the formation of plant-rich silica sinters. The sinters from Japan and their genesis will shed light on the origin and geological setting of similar deposits from the geological past.

CRediT authorship contribution statement

Aya Kubota: Writing – review & editing, Writing – original draft, Supervision, Project administration, Investigation, Funding acquisition, Conceptualization. **Ryo Taniguchi:** Writing – review & editing, Writing – original draft, Validation, Methodology, Investigation, Funding acquisition, Conceptualization. **Tomoyuki Ueda:** Writing – review & editing, Writing – original draft, Project administration, Methodology, Investigation, Funding acquisition, Data curation. **Yasuhiro Iba:** Writing – review & editing, Writing – original draft, Supervision, Project administration, Investigation, Funding acquisition, Conceptualization. All authors contributed equally to this work.

Declaration of competing interest

The authors declare that they have no known competing financial interests or personal relationships that could have appeared to influence the work reported in this paper.

Acknowledgements

We thank Jörg Mutterlose, Katsumi Matsuura, Harufumi Nishida, Yuichiro Kashiyama, Hitoshi Hasegawa, Yumi Sugahara, Hinata Matsumoto, and Nao Kawagoe for critical discussion; Takahito Momose, Agency for Cultural Affairs, and Azumino City Board of Education for granting permission to study Nakabusa Hot Springs; Kosuke Nakamura, and Hidehiko Nomura for sample preparation; Tomakomai Industrial Technology Center for supporting SEM analysis; Yohei Utsuki for the illustration in Fig. 6. This work was supported by the Japan Society for the Promotion of Science (grant number 23K27235 for A.K. and Y.I.; 22KJ0139 for R.T.; 23K17274 and 25K22459 for Y.I.); Pro Natura Foundation Japan 2023 and Chuo University Joint Research Grant for A. K.; Mont-bell Challenge Support Program 2023 for R.T.; Fukada Field Research Grant and Yuzawa Geopark Research Grant for U.T.; Japan Aerospace Exploration Agency (grant no. JX-PSPC-540452), Taisei Nature and History Fund 2024 and Ami Koshimizu Research Grant 2021 for Y.I.

Appendix A. Supplementary data

Supplementary data to this article can be found online at <https://doi.org/10.1016/j.palaeo.2025.113176>.

Data availability

All data are included in the manuscript and supplementary information files.

References

- Akahane, H., Yasuda, I., Miyajima, H., Goto, K., Honoki, H., 1997. Precipitation of silica sinter in hot spring water. *J. Geol. Soc. Jpn.* 103, 154–162 (in Japanese with English abstract). <https://doi.org/10.5575/geosoc.103.154>.
- Braunstein, D., Lowe, D.R., 2001. Relationship between spring and geyser activity and the deposition and morphology of high temperature (> 73 °C) siliceous sinter,

- Yellowstone National Park, Wyoming, U.S.A. *J. Sediment. Res.* 71, 747–763. <https://doi.org/10.1306/2DC40965-0E47-11D7-8643000102C1865D>.
- Cady, S.L., Skok, J.R., Gulick, V.G., Berger, J.A., Hinman, N.W., 2018. Siliceous hot spring deposits: Why they remain key astrobiological targets. In: Cabrol, N.A., Grin, E.A. (Eds.), *From Habitability to Life on Mars*. Elsevier, pp. 179–210. <https://doi.org/10.1016/B978-0-12-809935-3.00007-4>.
- Campbell, K.A., Sannazzaro, K., Rodgers, K.A., Herdianita, N.R., Browne, P.R.L., 2001. Sedimentary facies and mineralogy of the late Pleistocene Umukuri silica sinter, Taupo Volcanic Zone, New Zealand. *J. Sediment. Res.* 71, 727–746. <https://doi.org/10.1306/2DC40964-0E47-11D7-8643000102C1865D>.
- Campbell, K.A., Guido, D.M., Gautret, P., Foucher, F., Ramboz, C., Westall, F., 2015a. Geyserite in hot-spring siliceous sinter: window on Earth's hottest terrestrial (paleo) environment and its extreme life. *Earth Sci. Rev.* 148, 44–64. <https://doi.org/10.1016/j.earscirev.2015.05.009>.
- Campbell, K.A., Lynne, B.Y., Handley, K.M., Jordan, S., Farmer, J.D., Guido, D.M., Foucher, F., Turner, S., Perry, R.S., 2015b. Tracing biosignature preservation of geothermally silicified microbial textures into the geological record. *Astrobiology* 15, 858–882. <https://doi.org/10.1089/ast.2015.1307>.
- Channing, A., 2018. A review of active hot-spring analogues of Rhynie: environments, habitats and ecosystems. *Philos. Trans. R. Soc. B Biol. Sci.* 373, 20160490. <https://doi.org/10.1098/rstb.2016.0490>.
- Channing, A., Edwards, D., 2009a. Silicification of higher plants in geothermally influenced wetlands: Yellowstone as a lower Devonian Rhynie analog. *Palaios* 24, 505–521. <https://doi.org/10.2110/palo.2008.p08-131r>.
- Channing, A., Edwards, D., 2009b. Yellowstone hot-spring environments and the palaeo-ecophysiology of Rhynie chert plants: towards a synthesis. *Plant Ecol. Divers.* 2, 111–143. <https://doi.org/10.1080/17550870903349359>.
- Channing, A., Edwards, D., 2013. Wetland megabias: ecological and ecophysiological filtering dominates the fossil record of hot spring floras. *Palaeontology* 56, 523–556. <https://doi.org/10.1111/pala.12043>.
- Churchill, D.M., Manga, M., Hurwitz, S., Peek, S., Damby, D.E., Conrey, R., Wood, J.R., McCleskey, R.B., Keller, W.E., Hosseini, B., Hungerford, J.D.G., 2021. The structure and volume of large geyserites in Yellowstone National Park, USA, and the mineralogy and chemistry of their silica-sinter deposits. *J. Volcanol. Geotherm. Res.* 419, 107391. <https://doi.org/10.1016/j.jvolgeores.2021.107391>.
- Edwards, D., Kenrick, P., Dolan, L., 2018. History and contemporary significance of the Rhynie cherts—our earliest preserved terrestrial ecosystem. *Philos. Trans. R. Soc. B Biol. Sci.* 373, 20160489. <https://doi.org/10.1098/rstb.2016.0489>.
- Everroad, R.C., Otaki, H., Matsuura, K., Haruta, S., 2012. Diversification of bacterial community composition along a temperature gradient at a thermal spring. *Microbes Environ.* 27, 374–381. <https://doi.org/10.1264/jmee2.ME11350>.
- Fayers, S.R., Trewin, N.H., 2003. A review of the palaeoenvironments and biota of the Windyfield chert. *Earth Environ. Sci. Trans. R. Soc. Edinb.* 94, 325–339. <https://doi.org/10.1017/S0263593300000729>.
- Fernandez-Turiel, J.L., Garcia-Valles, M., Gimeno-Torrente, D., Saavedra-Alonso, J., Martinez-Manent, S., 2005. The hot spring and geyser sinters of El Tatio, Northern Chile. *Sediment. Geol.* 180, 125–147. <https://doi.org/10.1016/j.sedgeo.2005.07.005>.
- Garcia-Valles, M., Fernandez-Turiel, J.L., Gimeno-Torrente, D., Saavedra-Alonso, J., Martinez-Manent, S., 2008. Mineralogical characterization of silica sinters from the El Tatio geothermal field, Chile. *Am. Mineral.* 93, 1373–1383. <https://doi.org/10.2138/am.2008.2583>.
- Garwood, R.J., Oliver, H., Spencer, A.R., 2020. An introduction to the Rhynie chert. *Geol. Mag.* 157, 47–64. <https://doi.org/10.1017/S0016756819000670>.
- Gong, J., Munoz-Saez, C., Wilmet, D.T., Myers, K.D., Homann, M., Arp, G., Skok, J.R., van Zuilen, M.A., 2021. Morphogenesis of digitate structures in hot-spring silica sinters of the El Tatio geothermal field, Chile. *Geobiology* 20, 137–155. <https://doi.org/10.1111/gbi.12471>.
- Guido, D.M., Campbell, K.A., 2011. Jurassic hot spring deposits of the Deseado Massif (Patagonia, Argentina): characteristics and controls on regional distribution. *J. Volcanol. Geotherm. Res.* 203, 35–47. <https://doi.org/10.1016/j.jvolgeores.2011.04.001>.
- Guido, D.M., Channing, A., Campbell, K.A., Zamuner, A., 2010. Jurassic geothermal landscapes and fossil ecosystems at San Agustín, Patagonia, Argentina. *J. Geol. Soc. Lond.* 167, 11–20. <https://doi.org/10.1144/0016-76492009-109>.
- Guido, D.M., Campbell, K.A., Foucher, F., Westall, F., 2019. Life is everywhere in sinters: examples from Jurassic hot-spring environments of Argentine Patagonia. *Geol. Mag.* 156, 1631–1638. <https://doi.org/10.1017/S0016756819000815>.
- Gurdy, S.A., Chafetz, H.S., 2002. Factors governing subaqueous siliceous sinter precipitation in hot springs: examples from Yellowstone National Park, USA. *Sedimentology* 49, 1253–1267. <https://doi.org/10.1046/j.1365-3091.2002.00494.x>.
- Hamilton, A.R., Campbell, K.A., Rowland, J.V., Barker, S., Guido, D., 2019. Characteristics and variations of sinters in the Coromandel Volcanic Zone: application to epithermal exploration. *N. Z. J. Geol. Geophys.* 62, 531–549. <https://doi.org/10.1080/00288306.2018.1519514>.
- Hurwitz, S., Lowenstern, J.B., 2014. Dynamics of the Yellowstone hydrothermal system. *Rev. Geophys.* 52, 375–411. <https://doi.org/10.1002/2014RG000452>.
- Jones, B., Renaut, R.W., 2003. Hot spring and geyser sinters: the integrated product of precipitation, replacement and deposition. *Can. J. Earth Sci.* 40, 1549–1569. <https://doi.org/10.1139/e03-078>.
- Jones, B., Renaut, R.W., Rosen, M.R., 2003. Silicified microbes in a geyser mound: the enigma of low-temperature cyanobacteria in a high-temperature setting. *Palaios* 18, 87–109. [https://doi.org/10.1669/0883-1351\(2003\)18<87:SMIAGM>2.0.CO;2](https://doi.org/10.1669/0883-1351(2003)18<87:SMIAGM>2.0.CO;2).
- Kato, H., Sato, T., 1983. Geology of the Shinano-Ikeda district with geological sheet map at 1:50 000. In: Geological Survey of Japan, Tsukuba, 93 pp (in Japanese with English abstract).
- Kira, T., 1991. Forest ecosystems of east and Southeast Asia in a global perspective. *Ecol. Res.* 6, 185–200. <https://doi.org/10.1007/BF02347161>.
- Konhauser, K.O., Phoenix, V.R., Bottrell, S.H., Adams, D.G., Head, I.M., 2001. Microbial–silica interactions in Icelandic hot spring sinter: possible analogues for some Precambrian siliceous stromatolites. *Sedimentology* 48, 415–433. <https://doi.org/10.1046/j.1365-3091.2001.00372.x>.
- Konhauser, K.O., Jones, B., Reysenbach, A.L., Renaut, R.W., 2003. Hot spring sinters: keys to understanding Earth's earliest life forms. *Can. J. Earth Sci.* 40, 1713–1724. <https://doi.org/10.1139/e03-059>.
- Kubo, K., Knittel, K., Amano, R., Fukui, M., Matsuura, K., 2011. Sulfur-metabolizing bacterial populations in microbial mats of the Nakabusa hot spring, Japan. *Syst. Appl. Microbiol.* 34, 293–302. <https://doi.org/10.1016/j.syapm.2010.12.002>.
- Lowe, D.R., Braunstein, D., 2003. Microstructure of high-temperature (> 73 °C) siliceous sinter deposited around hot springs and geysers, Yellowstone National Park: the role of biological and abiological processes in sedimentation. *Can. J. Earth Sci.* 40, 1611–1642. <https://doi.org/10.1139/e03-066>.
- Lynne, B.Y., Campbell, K.A., 2004. Morphologic and mineralogic transitions from Opal-A to Opal-CT in low-temperature siliceous-sinter diagenesis, Taupo Volcanic Zone, New Zealand. *J. Sediment. Res.* 74, 561–579. <https://doi.org/10.1306/011704740561>.
- Lynne, B.Y., Boudreau, A., Smith, I.J., Smith, G.J., 2019. Silica accumulation rates for siliceous sinter at Orakei Korako geothermal field, Taupo Volcanic Zone, New Zealand. *Geothermics* 78, 50–61. <https://doi.org/10.1016/j.geothermics.2018.11.007>.
- Matsumoto, T., Yamada, R., Iizuka, S., 2022. Heat flow data and thermal structure in northeastern Japan. *Earth Planets Space* 74, 155. <https://doi.org/10.1186/s40623-022-01704-4>.
- Ministry of Land, Infrastructure, Transport and Tourism (MLIT), 2022. Digital National Land Information, Version 2022 [Dataset]. National Land Numerical Information download service. Government of Japan. Available at: <https://nlftp.mlit.go.jp/ksj/gml/datalist/KsjTmpl-G02-2022.html> (accessed 26 May 2025).
- Mountain, B.W., Benning, L.G., Boerema, J.A., 2003. Experimental studies on New Zealand hot spring sinters: rates of growth and textural development. *Can. J. Earth Sci.* 40, 1643–1667. <https://doi.org/10.1139/e03-068>.
- Nakada, S., 2017. Volcanic archipelago: Volcanism as a geoheritage characteristic of Japan. In: Yamamoto, S. (Ed.), *Natural Heritage of Japan: Geological, Geomorphological, and Ecological Aspects*. Springer, Cham, pp. 19–28. https://doi.org/10.1007/978-3-319-61896-8_3.
- Nakagawa, T., Fukui, M., 2002. Phylogenetic characterization of microbial mats and streamers from a Japanese alkaline hot spring with a thermal gradient. *J. Gen. Appl. Microbiol.* 48, 211–222. <https://doi.org/10.2323/jgam.48.211>.
- Nicolau, C., Reich, M., Lynne, B., 2014. Physico-chemical and environmental controls on siliceous sinter formation at the high-altitude El Tatio geothermal field, Chile. *J. Volcanol. Geotherm. Res.* 282, 60–76. <https://doi.org/10.1016/j.jvolgeores.2014.06.012>.
- Ozaki, K., 1972. Plant fossils from the siliceous sinters in Sokokura, Hakone-Machi, Kanagawa Prefecture, Japan. *Sci. Rep. Yokohama Natl. Univ., Sect. 2, Biol. Sci.* 19, 159–169 (in Japanese with English abstract).
- Renaut, R.W., Jones, B., Tiercelin, J.J., Tarits, C., 2002. Sublacustrine precipitation of hydrothermal silica in rift lakes: evidence from Lake Baringo, Central Kenya Rift Valley. *Sediment. Geol.* 148, 235–257. [https://doi.org/10.1016/S0037-0738\(01\)00220-2](https://doi.org/10.1016/S0037-0738(01)00220-2).
- Rice, C.M., Trewin, N.H., Anderson, L.I., 2002. Geological setting of the early Devonian Rhynie cherts, Aberdeenshire, Scotland: an early terrestrial hot spring system. *J. Geol. Soc. Lond.* 159, 203–214. <https://doi.org/10.1144/0016-764900-181>.
- Rowe, M.C., Campbell, K.A., Hamilton, A., Jiang, Y., Pelsner, J., Murphy, B., Martin, R., Mackenzie, K.M., Stallard, D.A., Lyon, B., Langendam, A., Nersezoza, E.E., Guido, D. M., Rowland, J.V., 2025. Life and death of a sinter archive: Evolution of siliceous hot-spring deposits (Holocene) on the dynamic Paeroa Fault at Te Kopia, Taupo Volcanic Zone, New Zealand. *J. Volcanol. Geotherm. Res.* 465, 108380. <https://doi.org/10.1016/j.jvolgeores.2025.108380>.
- Ruff, S.W., Farmer, J.D., 2016. Silica deposits on Mars with features resembling hot spring biosignatures at El Tatio in Chile. *Nat. Commun.* 7, 13554. <https://doi.org/10.1038/ncomms13554>.
- Sagasti, A.J., Campbell, K.A., García Massini, J.L., Galar, A., Guido, D.M., Gautret, P., 2024. Fossil geyserite and testate amoebae in geothermal spring vent pools: Paleogeology and variable preservation quality in Jurassic sinter of Patagonia (Deseado Massif, Argentina). *Geobiology* 22, e12621. <https://doi.org/10.1111/gbi.12621>.
- Sato, D., 1922. Hot springs with siliceous sinter in Japan. *J. Geol. Soc. Tokyo* 29, 186–198. <https://doi.org/10.5575/geosc.29.186>.
- Squyres, S.W., Arvidson, R.E., Ruff, S., Gellert, R., Morris, R.V., Ming, D.W., Crumpler, L., Farmer, J.D., Des Marais, D.J., Yen, A., McLennan, S.M., Calvin, W., Bell III, J.F., Clark, B.C., Wang, A., McCoy, T.J., Schmidt, M.E., de Souza Jr., P.A., 2008. Detection of silica-rich deposits on Mars. *Science* 320, 1063–1067. <https://doi.org/10.1126/science.1155429>.
- Strullu-Derrien, C., Kenrick, P., Knoll, A.H., 2019. The Rhynie chert. *Curr. Biol.* 29, R1218–R1223. <https://doi.org/10.1016/j.cub.2019.10.030>.
- Suzuki, T., 1889. Geology lecture 3. *J. Geogr.* 1, 358–371. <https://doi.org/10.5026/jgeography.1.358>.
- Taira, A., 2001. Tectonic evolution of the Japanese island arc system. *Annu. Rev. Planet. Sci.* 29, 109–134. <https://doi.org/10.1146/annurev.earth.29.1.109>.

- Tobler, D., Stefánsson, A., Benning, L.G., 2008. In-situ grown silica sinters in Icelandic geothermal areas. *Geobiology* 6, 481–502. <https://doi.org/10.1111/j.1472-4669.2008.00179.x>.
- Trewin, N.H., Kerp, H., 2017. The Rhynie and Windyfield cherts, early Devonian, Rhynie, Scotland. In: Brayard, A., Escarguel, G. (Eds.), *Terrestrial Conservation Lagerstätten: Windows into the Evolution of Life on Land*. Elsevier, Amsterdam, pp. 1–38. <https://doi.org/10.2307/jj.12638994.4>.
- Trewin, N.H., Rice, C.M. (Eds.), 2004. *The Rhynie Hot-Spring System: Geology, Biota and Mineralisation*. The Royal Society of Edinburgh Scotland Foundation, Edinburgh, 246 pp.
- Walter, M.R., Desmarais, D., Farmer, J.D., Hinman, N.W., 1996. Lithofacies and biofacies of mid-Paleozoic thermal-spring deposits in the Drummond Basin, Queensland, Australia. *Palaeos* 11, 497–518. <https://doi.org/10.2307/3515187>.
- Wellman, C.H., 2018. Palaeoecology and palaeophytogeography of the Rhynie chert plants: further evidence from integrated analysis of *in situ* and dispersed spores. *Philos. Trans. R. Soc. B Biol. Sci.* 373, 20160491. <https://doi.org/10.1098/rstb.2016.0491>.
- White, D.E., Brannock, W.W., Murata, K.J., 1956. Silica in hot-spring waters. *Geochim. Cosmochim. Acta* 10, 27–59. [https://doi.org/10.1016/0016-7037\(56\)90010-2](https://doi.org/10.1016/0016-7037(56)90010-2).
- White, N.C., Wood, D.G., Lee, M.C., 1989. Epithermal sinters of Paleozoic age in North Queensland, Australia. *Geology* 17, 718–722. [https://doi.org/10.1130/0091-7613\(1989\)017<0718:ESOPAI>2.3.CO;2](https://doi.org/10.1130/0091-7613(1989)017<0718:ESOPAI>2.3.CO;2).
- You, Y., Wen, H., Luo, L., Campbell, K.A., Guido, D.M., Capezzuoli, E., Lu, Z., Du, L., Yang, Y., 2024. A cretaceous siliceous sinter in NE China: Sedimentological and geochemical constraints on its genesis. *Sediment. Geol.* 464, 106618. <https://doi.org/10.1016/j.sedgeo.2024.106618>.